

Research Article

Fabrication and Properties of Stainless-Steel Foams with Simultaneous Use of Two Different Space Holders

Z. Shojaei and M.H. Paydar*

Department of Materials Science and Engineering, School of Engineering, Shiraz University, Shiraz, Iran

ARTICLE INFO

Article history:

Received 20 January 2025

Reviewed 11 February 2025

Revised 13 February 2025

Accepted 16 February 2025

Keywords:

Carbamide

Metal foam

Powder space holder technique

Steel hollow sphere

316L stainless steel

Please cite this article as:

Shojaei, Z., & Paydar, M. H. (2024). Fabrication and properties of stainless-steel foams with simultaneous use of two different space holders. *Iranian Journal of Materials Forming*, 11(4), 45-51. <https://doi.org/10.22099/IJMF.2025.52230.1319>

ABSTRACT

In this study, low-density yet high-strength 316L stainless steel foam was successfully fabricated using the powder metallurgy technique. This was achieved by employing both carbamide and steel hollow spheres as space holders to tailor porosity and mechanical properties. The volumetric percentage of carbamide was varied from 0 to 50% to investigate its effect on density, while steel hollow spheres (0%–50% by volume) were incorporated to enhance strength. The fabrication process involved layer-by-layer deposition of stainless steel powder and space holders in a mold, followed by uniaxial compaction at 150 MPa using polyvinyl alcohol as a binder. Carbamide was removed through heat treatment at 120–180 °C in ambient conditions, and the samples were subsequently sintered at 1150 °C for 3 hours in a neutral atmosphere. Following optimization of fabrication parameters and porosity control, the samples were characterized using compression tests and scanning electron microscopy (SEM) to evaluate their mechanical performance and microstructural evolution. Compression test results revealed that increasing carbamide content decreased the density, whereas a higher percentage of steel hollow spheres significantly improved compressive strength, reaching a maximum of 528.70 MPa at constant porosity. SEM analysis confirmed that the replacement of carbamide with steel hollow spheres led to the transformation of open-cell porosity into closed-cell porosity.

© Shiraz University, Shiraz, Iran, 2024

1. Introduction

Metal foams are a specialized class of cellular structures composed of metals with an interconnected network of pores [1]. Their lightweight nature, high specific stiffness, impressive strength-to-weight ratios, and exceptional energy-absorbing capabilities make them ideal for applications in the automotive, biomedical, and aerospace industries [2, 3]. Various metals have been

utilized in metal foam fabrication, including titanium, titanium alloys, copper, nickel, aluminum, magnesium, and stainless steel [4-6]. Among these, steel foams are often preferred due to their higher elastic modulus, yield strength, and operating temperature. However, manufacturing steel foams remains challenging [7, 8].

A crucial aspect of metal foam fabrication is

* Corresponding author

E-mail address: paaydar@shirazu.ac.ir (M. H. Paydar)<https://doi.org/10.22099/IJMF.2025.52230.1319>

selecting an appropriate spacer material that is easily soluble or removable by heat. Carbamide space holders (urea, $(\text{NH}_2)_2\text{CO}$) are widely used as a space holder due to their high solubility in water, affordability, and availability in various sizes and shapes [9-11].

Bekoz et al. [12] successfully produced highly porous steel foam using carbamide as a space holder. They employed both spherical and irregular-shaped carbamide particles, which were later removed through a water leaching technique. Their findings indicated that using irregular carbamide particles required shorter leaching time. Furthermore, the degree of volumetric expansion (after carbamide leaching) and volumetric shrinkage (after sintering) depended on both the volume fraction and shape of the carbamide. Additionally, foams with spherical pores exhibited better compressive behavior due to their smooth-walled cell structure, whereas foams with irregular pores experienced stress concentrations at sharp edges, leading to lower strength.

Similarly, Mirzaei et al. [13] developed porous 316L stainless steel (SS 316L) with a uniform pore distribution using face-centered cubic (FCC) packing achieved with spherical carbamide as the space holder. Their results demonstrated that a uniform pore distribution enhances both elastic properties and compressive strength.

However, the impact of simultaneously using two different types of space holders—one removable and the other unremovable—on the mechanical properties of metallic foam remains unexplored. Therefore, this study aims to fabricate stainless steel foam using powder metallurgy, incorporating both carbamide (removable) and hollow steel spheres (unremovable) as space holders. The study further investigates the mechanical properties and energy absorption of these foams to determine the optimal combination of carbamide and hollow spheres for steel foam construction.

2. Experimental Procedure

2.1. Materials

Stainless steel (316L) powder, with a mean particle size of $37 \mu\text{m}$ and a density of 8 g/cm^3 , was supplied by Carpenter Sweden Co. The chemical composition of the stainless steel powder is presented in Table 1.

Hollow steel spheres, with a diameter of 2 mm and a density of 0.43 g/cm^3 , were used as a space holder. The chemical composition of the spheres as provided by the supplier (Fraunhofer Co.), is summarized in Table 2.

As the second space holder, commercially available spherical carbamide in the 1700–2400 μm size range, with a sphericity of 0.94, was used. Additionally, 6 wt.% polyvinyl alcohol (Merck Co.) was employed as a binder, and 0.5 wt.% boron (Sigma Aldrich Co.) was added to enhance the sintering process. Fig. 1 presents images of the SS 316L powder, hollow steel spheres, and carbamide particles used in this study.

2.2. Steel foam manufacturing procedure

To fabricate stainless steel foam, steel powder was first mixed with boron, followed by the addition of polyvinyl alcohol as a binder. The mixing process was carried out manually using a mortar. The resulting mixture was then compacted uniaxially in a steel die ($d=22 \text{ mm}$), with space holders incorporated as required.

Table 1. Chemical composition of the stainless steel (316L) powder

Elements	Fe	Ni	Mn	Cr	Si	Mo	C
wt.%	bal	10	1.1	15.58	1.08	4.32	7.24

Table 2. Chemical composition of the hollow steel spheres

Elements	Fe	O	C
wt.%	bal	0.002	0.007

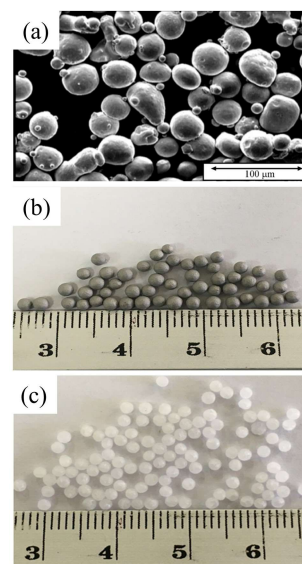


Fig. 1. Images of (a) SS 316L powder, (b) iron hollow spheres, and (c) carbamides used in this study.

The fabrication process involved adjusting the punch height within the die, pouring and leveling the steel powder onto the lower punch, and carefully placing carbamide and hollow steel sphere particles in designated spots. This layering process was repeated until the desired foam dimensions ($h=22$ to 25 mm) were achieved. Further details of the fabrication method can be found elsewhere [13]. The green specimens were produced by uniaxially pressing the mixture at 150 MPa using a hydraulic press. The final stage of the process involved heat treatment, conducted in two stages within a tube furnace. In the first stage, carbamide decomposition occurred at a temperature range of 120 - 180 °C. The second stage involved sintering the SS 316L compacted metal powder at 1150 °C for 2 hours under an argon (Ar) atmosphere.

Following foam production, microstructure of the metal foam was analyzed using scanning electron microscopy (SEM, VEGA TESCAN). The density and residual porosity of the specimens were determined by measuring their volume, dimensions, and weights. Compression testing was conducted in accordance with the ASTM E9–89a standard using a universal testing machine (SANTAM) at a crosshead speed of 0.5 mm/min. The absorbed energy was calculated by evaluating the area under the stress-strain curve.

3. Results and Discussion

3.1. Foam structure

Figs. 2(a) and 2(b) illustrate the microstructure of SS 316L foam, depicting the cellular structure and the detailed morphology of the cell walls, respectively.

As illustrated in Fig. 2(a), the foam structure consists of both open-cell and closed-cell porosity. Open-cell porosity results from the removal of carbamide during heat treatment, while the steel hollow spheres contribute to a closed cell structure, as they remain embedded within the material. Fig. 2(b) further illustrates the well-defined cell walls separating adjacent pores. This combination of open and closed porosity makes the foam highly suitable for applications requiring the advantages of both structures, such as lightweight energy-absorbing materials, heat exchangers, and biomedical implants.

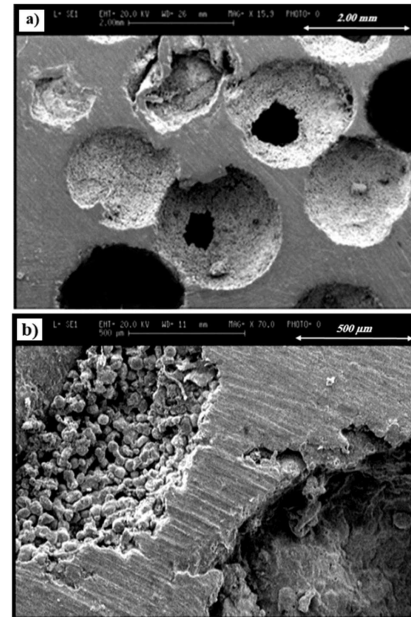


Fig. 2. SEM image of SS 316L foam manufactured using two different space holders: (a) foam cells and (b) cell walls.

3.2. Foam density

The relative density of foam is defined as:

$$\rho_{th} = v_{ss}\rho_{ss} + v_{HS}\rho_{HS} \quad (1)$$

$$v_{ss} = 1 - (v_{HS} + v_{CB}) \quad (2)$$

Where, ρ_{th} is the theoretical density of the foam, ρ_{ss} and ρ_{HS} , are the densities of the 316L stainless steel powder and the steel hollow spheres, respectively and v_{ss} , v_{HS} and v_{CB} represent the volumetric fraction of 316L stainless steel powder, steel hollow sphere and carbamide, respectively.

As previously mentioned, carbamide is removed from the specimen during the heating process. Consequently, the theoretical density is calculated considering only the steel hollow spheres and stainless steel powder, though their combined volumetric fraction does not equal one. To determine the actual density of the foam, the mass and volume of each specimen were measured, and the density was obtained by dividing the mass by the volume. The relative density of metal foams, defined as the ratio of foam density to the density of the base material, is a crucial parameter that highlights the lightweight characteristics of the foam. Table 3 provides detailed information on the density measurement of

316L stainless steel foams with 50% porosity, fabricated using both carbamide and hollow steel spheres.

Fig. 3 illustrates the impact of steel hollow spheres on both theoretical and actual (measured) density. Analyzing this figure alongside Table 3 reveals a noticeable difference between the actual density and the theoretical density of the foam. This discrepancy may arise from porosity in the base metal due to carbamide removal, deformation of the steel hollow spheres, and measurement errors. Both theoretical and actual densities increase in proportion to the amount of steel hollow spheres relative to carbamide. Since this study focuses on foam with 50% volumetric porosity, the volumetric percentage of the stainless steel powder remains constant, while only the amounts of carbamide and steel hollow spheres vary.

As the percentage of steel hollow spheres increases, both theoretical and actual densities rise. This occurs because carbamide is removed, leaving the steel hollow spheres embedded in the specimen. The final structure results in a composite-like metal foam, where the retained steel hollow spheres contribute to the overall mechanical integrity of the material.

Fig. 4 illustrates the impact of the percentage of steel hollow spheres on relative density, while Fig. 5 depicts the effect of steel hollow spheres on the ratio of actual density to theoretical density. As shown in Figs. 4 and 5, increasing the volumetric percentage of steel hollow spheres relative to carbamide leads to a rise in both the relative density and the ratio of actual density to theoretical density. This trend can be attributed to the removal of carbamide, which leaves behind the steel hollow spheres, forming a composite foam. However, during the compression test, some steel hollow spheres may shift, causing discrepancies between actual and

theoretical densities and affecting the overall density ratio.

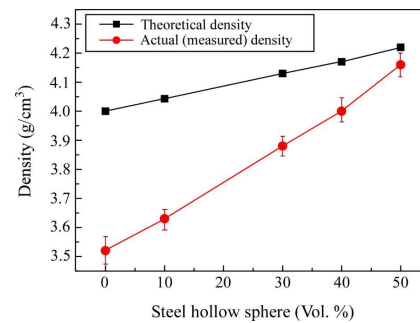


Fig. 3. The effect of the volumetric percentage of steel hollow spheres on the theoretical and actual density of the produced foams.

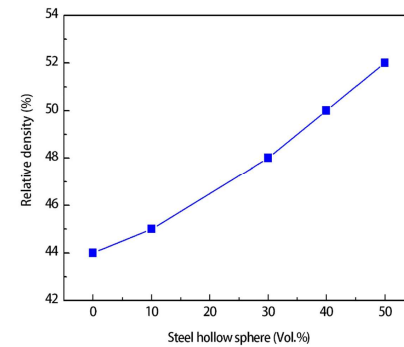


Fig. 4. The effect of the volumetric percentage of steel hollow spheres on the relative density of the formed foams.

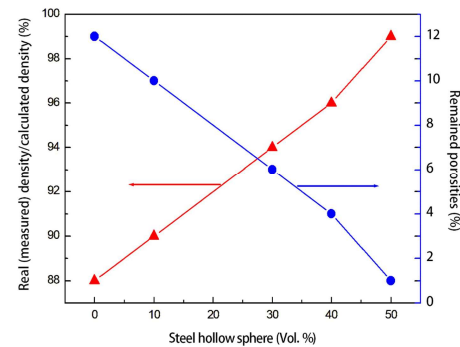


Fig. 5. The effect of the volumetric percentage of the steel hollow sphere on the ratio of actual density to theoretical density in the produced foams.

Table 3. Density of SS 316L foams made using both types of space holders

Hollow sphere (vol.%)	Carbamide (vol.%)	Theoretical density (g/cm ³)	Real (measured) density (g/cm ³)	Real (measured) density/calculated density %	Relative density (with respect to ρ_{th} of SS) %	Remained porosities %
0	50	4	3.52	88	44	56
10	40	4.043	3.63	90	45	55
30	20	4.13	3.88	94	48	52
40	10	4.17	4	96	50	50
50	0	4.22	4.16	99	52	48

3.3. Effect of porosity on carbamide removal efficiency

To investigate the effect of porosity on the efficiency of carbamide removal, two conditions were established. In condition one, the volume percentage of steel hollow spheres remains constant at 20%, while the volume percentage of carbamide is variable. In condition two, the volumetric percentage of steel hollow spheres is variable, while the volume percentage of carbamide remains constant at 20%.

Figs. 6(a) and 6(b) illustrate the effects of the amount of remaining porosity on the percentage of carbamide that could be removed under conditions where the volumetric percentages of steel hollow spheres and carbamide remain constant, respectively. Fig. 6a demonstrates that as the volume percentage of carbamide increases, its removal rate also increases. Conversely, Fig. 6(b) indicates that as the volume percentage of steel hollow spheres increases, the removal of carbamide decreases. This occurs because the pores created by steel hollow spheres are predominantly closed-cell, which obstructs the pathway necessary for efficient carbamide removal.

3.4. Investigating the compressive behavior

Fig. 7 presents the stress-strain curve of samples with 50% volumetric porosity, incorporating varying percentages of carbamide and steel hollow spheres. The curve was used to determine the yield strength, the slope of the elastic region, the plateau region stress, and the compressive strength.

As shown in Fig. 7 and Table 4, an increase in the volumetric percentage of steel hollow spheres relative to carbamide at 50% volumetric porosity leads to a corresponding increase in yield strength, the slope of the elastic region, plateau region stress, and compressive strength. This phenomenon occurs because, as

previously mentioned, the steel hollow spheres create closed-cell type porosities, which are more resistant compared to carbamide-based porosities and generally exhibit superior compressive properties.

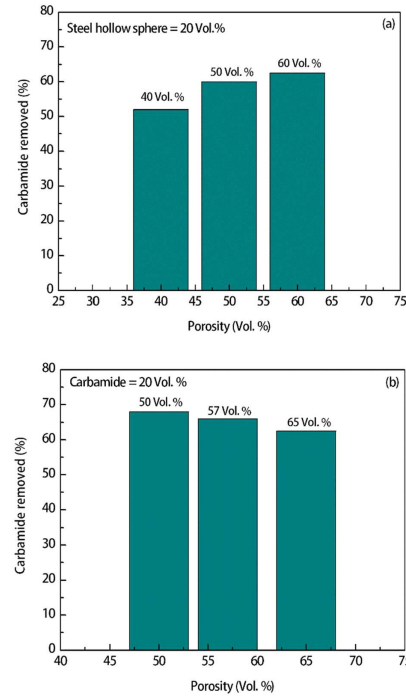


Fig. 6. Effect of porosity on carbamide removal in condition (a) by increasing porosity due to an increase in carbamide and (b) by increasing porosity due to an increase in steel hollow spheres.

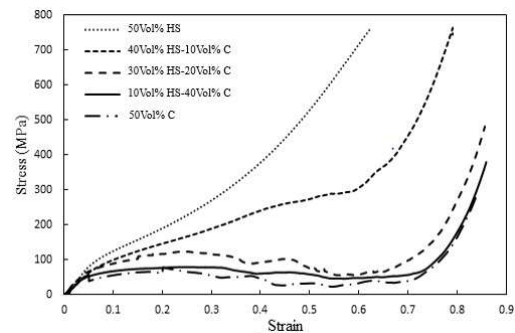


Fig. 7. Stress-strain curves were generated for samples with 50% porosity, incorporating varying volumetric percentages of carbamide and steel hollow spheres.

Table 4. Mechanical properties derived from the stress-strain curve

Carbamide (vol.%)	Hollow sphere (vol.%)	Yield strength (MPa)	Elastic region slope (GPa)	Compressive strength (MPa)	Plateau region stress (MPa)
50	0	38	2.10	84	38
40	10	45	2.32	90	60.08
20	30	55	2.59	106.21	83
10	40	69.7	2.64	297.29	197.82
0	50	82	2.73	528.70	269.36

3.5. Energy absorption

The energy absorbed by the samples was determined by calculating the area under the stress-strain curve. Table 5 shows the energy absorption values for samples with 50 vol.% porosity, incorporating different volumetric percentages of carbamide and steel hollow spheres, up to a strain of 0.5. Beyond this strain level, densification occurs due to compression.

As shown in Table 5, an increase in the percentage of steel hollow spheres leads to a decrease in compressive strain while energy absorption increases. This is attributed to the rise in both compressive strength and plateau region stress in the stress-strain curve.

Fig. 8 illustrates the energy absorption efficiency curve for samples with 50 vol.% porosity, containing varying amounts of carbamide and steel hollow spheres. The energy absorption efficiency is calculated using Eq. (3) [14].

$$\eta = E / (\sigma_m \cdot \varepsilon_m) \quad (3)$$

$$E = \int_0^{\varepsilon} \sigma(\varepsilon) d\varepsilon \quad (4)$$

Where η represents energy absorption efficiency, E is the amount of absorbed energy, σ_m indicates maximum stress, and ε signifies strain. Energy absorption efficiency measures how much energy a material absorbs up to a certain strain relative to the maximum energy absorbed before failure.

The energy absorption efficiency curve is divided into three regions: a sharp increase (Region I) where the energy absorption efficiency rises sharply with increasing strain, reaching its peak; a sustained region (Region II) where the energy absorption efficiency remains high but exhibits occasional fluctuations, indicating foam instability during compression. In the weakening region (Region III), the energy absorption efficiency drops significantly as strain increases [15, 16]. As depicted in Fig. 8, samples containing more than 20 vol. % carbamide demonstrate an energy absorption efficiency exceeding 75%, with peak efficiency occurring at strains between 0.2 and 0.5. Notably, samples with 50 and 40 vol.% carbamide display the

longest sustained region. Conversely, specimens containing 50 and 40 vol.% of steel hollow spheres demonstrate lower energy absorption efficiency, likely due to their high compressive strength.

Table 5. Energy absorbed by samples with 50% porosity and various carbamide content and steel hollow spheres

Carbamide (vol.%)	Hollow sphere (vol.%)	Compressive strain	Energy absorption (MJ/m ³)
50	0	0.75	38.10
40	10	0.74	48
20	30	0.69	83
10	40	0.58	107.80
0	50	0.5	123.09

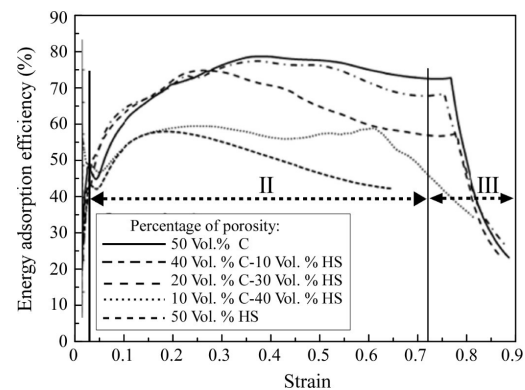


Fig. 8. Energy absorption curve of sample with 50% porosity and various carbamide and steel hollow sphere content.

4. Conclusions

In this study, stainless steel 316L foam was successfully fabricated using two types of space holders: steel hollow spheres and carbamide. The compressive properties of the produced foams were analyzed and compared. The key findings are summarized as follows:

1. The incorporation of carbamide into the steel foam structure leads to the formation of open-cell porosity, whereas steel hollow spheres create closed-cell porosity.
2. An increase in the percentage of steel hollow spheres results in more closed-cell porosities, which hinders the removal of carbamide at temperatures between 120 °C and 180 °C.
3. In foams with 50 vol.% porosity, a higher percentage of steel hollow spheres enhances yield strength, increases the stiffness of the elastic region, and improves overall compressive strength.

4. Increasing the steel hollow sphere content to 50 vol.% significantly enhances energy absorption while reducing compressive strain.

Acknowledgments

The authors gratefully acknowledge Shiraz University for providing financial support during the research work.

Conflict of interest

The authors declare no conflict of interest.

Funding

This research was funded by Shiraz University.

5. References

- [1] Banhart, J. (1999). Foam metal: the recipe. *Europhysics News*, 30(1) 17-20. <https://doi.org/10.1007/s00770-999-0017-8>
- [2] Pérez, L., Mercado, R., & Alfonso, I. (2017). Young's modulus estimation for CNT reinforced metallic foams obtained using different space holder particles. *Composite Structures*, 168, 26-32. <https://doi.org/10.1016/j.compstruct.2017.02.017>
- [3] Mutlu, I., & Oktay, E. (2011). Production and characterization of Cr-Si-Ni-Mo steel foams. *Indian Journal of Engineering and Materials Science*, 18(3), 227-232. <http://nopr.niscares.in/handle/123456789/12470>
- [4] Rosip, N. M., Ahmad, S., Jamaludin, K., & Noor, F. M. (2013). Producing of 316L stainless steel (SS 316L) foam via slurry method. *Journal of Mechanical Engineering and Sciences*, 5, 707-712. <https://doi.org/10.15282/jmes.5.2013.17.0068>
- [5] Besharati, F., & Paydar, M. H. (2023). Fabrication of copper open cell foam by electrochemical deposition method and investigation on the effect of current intensity and plating solution on the created microstructure. *Iranian Journal of Materials Forming*, 10(1), 4-12. <https://doi.org/10.22099/ijmf.2023.46551.1245>
- [6] Hassanli, F., & Paydar, M. H. (2022). Effect of green body formation by single and double action pressing on the mechanical properties of Al foams. *Iranian Journal of Materials Forming*, 9(1) 5-12. <https://doi.org/10.22099/ijmf.2022.42018.1197>
- [7] Smith, B., Szyniszewski, S., Hajjar, J., Schafer, B., & Arwade, S. (2011). Steel foam for structures: A review of applications, manufacturing and material properties. *Journal of Constructional Steel Research*, 71, 1-10. <https://doi.org/10.1016/j.jcsr.2011.10.028>
- [8] Babcsán, N., Banhart, J., & Leitmeier, D. (2003, November). Metal foams—manufacture and physics of foaming. In *Proceedings of the International Conference Advanced Metallic Materials* (Vol. 5, p. 15).
- [9] Nakajima, H., Hyun, S. K., Park, J. S., Tane, M. (2007, February). Fabrication of louts-type porous petals by continuous zone pelting and continuous casting techniques. In *Materials Science Forum* (Vol. 539, pp. 187-192). Trans Tech Publications Ltd. <https://doi.org/10.4028/www.scientific.net/MSF.539-543.187>
- [10] Rabiei, A., & Vendra, L. (2009). A comparison of composite metal foam's properties and other comparable metal foams. *Materials Letters*, 63(5), 533-536. <https://doi.org/10.1016/j.matlet.2008.11.002>
- [11] Stanev, L., Kolev, M., Drenchev, B., & Drenchev, L. (2017). Open-cell metallic porous materials obtained through space holders—Part II: structure and properties. a review. *Journal of Manufacturing Science and Engineering*, 139(5), 050802-050833. <https://doi.org/10.1115/1.4034440>
- [12] Bekoz, N., & Oktay, E. (2012). Effects of carbamide shape and content on processing and properties of steel foams. *Journal of Materials Processing Technology*, 212(10), 2109-2116. <https://doi.org/10.1016/j.jmatprotec.2012.05.015>
- [13] Mirzaei, M., & Paydar, M. H. (2017). A novel process for manufacturing porous 316 L stainless steel with uniform pore distribution. *Materials & Design*, 121(5), 442-449. <https://doi.org/10.1016/j.matdes.2017.02.069>
- [14] Besharati, F., & Paydar, M. H. (2024). Investigation on the microstructure and compressive behavior of open-cell copper-Al₂O₃ composite foams. *Journal of Materials Research and Technology*, 33, 3427–3438. <https://doi.org/10.1016/j.jmrt.2024.10.059>
- [15] Xia, X. C., Chen, X. W., Zhang, Z., Chen, X., Zhao, W. M., Liao, B. & Hur, B. (2013). Effects of porosity and pore size on the compressive properties of closed-cell Mg alloy foam. *Journal of Magnesium and Alloys*, 1(4), 330-335. <https://doi.org/10.1016/j.jma.2013.11.006>
- [16] Hassanli, F., & Paydar, M. H. (2021). Improvement in energy absorption properties of aluminum foams by designing pore-density distribution. *Journal of Materials Research and Technology*, 14, 609–619. <https://doi.org/10.1016/j.jmrt.2021.06.073>